PHYSICAL REVIEW A VOLUME 23, NUMBER 6 JUNE 1981

Transient analysis of Kerr-like phase conjugators using frequency-domain techniques

Robert A. Fisher, B. R. Suydam, and B. J. Feldman
University of California, Los Alamos Scientific Laboratory, Los Alamos, New Mexico 87545
(Received 5 September 1980)

In this paper we develop the interrelationships between the steady-state and transient behavior for cw-pumped Kerr-like conjugators in which the optical Kerr effect is considered to respond instantaneously. We use Laplace-transform techniques to develop an expression for the conjugate response to input pulses of arbitrary form. For stable conjugator operation (in which the cw conjugate reflectivity is finite for all input frequencies), the expression reduces to an antilinear Fourier-transform relationship, which is readily adaptable to computer simulation. The cw filter function of Pepper and Abrams [Opt. Lett. 3, 312 (1978)] is found to play a central role. We show, both numerically and analytically, that our calculated delta-function response agrees with that previously published. We numerically demonstrate temporal spreading and reshaping when the conjugator transit time becomes equal to or longer than the duration of the input pulse, and we show numerically the perfect chirp reversal for sufficiently thin conjugators and the deviations from perfect chirp reversal upon increasing the thickness of the conjugator. These numerical results can be understood in terms of the bandwidth of the associated cw filter function.

I. INTRODUCTION

A. General

Optical phase conjugation (or "wave-front reversal") via degenerate four-wave mixing in Kerr-like media has recently become an extremely popular subject. The unusual "aberration-free" image transformation properties of phase conjugators suggest many practical applications in fields as diverse as adaptive optics, laser fusion, image restoration, real-time holography, high-resolution microscopy, and optical computing.

Although there are many early publications which, in retrospect, contain concepts that clearly establish the basis for conjugation via Kerr-like degenerate four-wave mixing,[1] Hellwarth[2] was the first to explore the image transformation properties and to quantify the nature of the nonlinear interaction. In the process, he stimulated much subsequent work. The setup discussed in Ref. 2 is shown in Fig. 1. A pair of precisely counterpropagating but arbitrarily oriented cw plane waves (called "pump waves") is established in an optical Kerr material (one in which the index of refraction depends linearly upon the optical intensity). Both pump waves have the same carrier frequency. If a third weaker cw-probe wave (E_p in the figure) at nearly the same carrier frequency also impinges upon the material, the nonlinear interaction creates a fourth cw conjugate wave (E_c in the figure) which exactly retraces the path of E_p. The production of the conjugate wave can be thought of as a real-time holographic process[3]; the probe wave and each pump wave interfere in the nonlinear medium to generate a grating which is properly phase matched to Bragg scatter the other pump wave into the conjugate direction.

B. Steady-state theory

Bjorklund and Bloom[3] and Yariv and Pepper[4] concurrently developed a steady-state coupled-wave theory of Kerr-like conjugators in which all four waves were at precisely the same frequency (the *degenerate* case). They found the "conjugate reflectivity" (the ratio of the conjugate wave *intensity* to the probe wave *intensity*) to be $\tan^2(|\kappa| l)$. For the case of equal-intensity pumps $|\kappa| = (2\pi/\lambda_0)\delta n$, l is the path length over which the pump and probe waves interact in the nonlinear medium. Here λ_0 is the free-space wavelength of the light, and δn is the nonlinear refractive index change induced by *one* pump wave. Shortly after the development of this cw degenerate theory, many corroborating experiments were reported.[1,5]

Pepper and Abrams[6] subsequently relaxed the

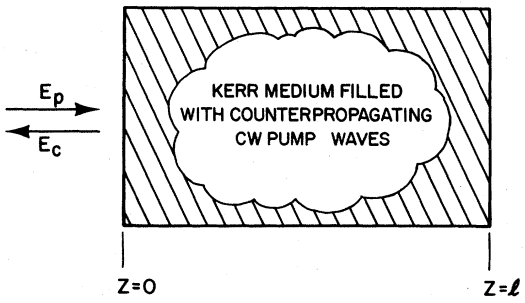

FIG. 1. The basic arrangement for obtaining conjugation via four-wave mixing in Kerr media. The Kerr medium is pumped by a pair of cw counterpropagating waves of common frequency. The probe wave E_p impinges upon the medium, and the medium reradiates a conjugate wave E_c. The arrows denote the directions of the corresponding k vectors.

degeneracy condition by allowing the cw-probe wave to be at a frequency different from that of the cw pump waves. The resulting conjugate wave is frequency upshifted (or downshifted) by precisely the amount by which the probe wave is downshifted (or upshifted). The conjugate-wave amplitude was shown to be the complex conjugate of the input wave amplitude multiplied by a complex filter function. It is a slight variant of this cw antilinear transfer function that we will find central to our development of the conjugator's transient response.

C. Transient theory

Marburger[7] was the first to study theoretically the conjugation of time-varying pulses. He explored the time-domain behavior of the pair of coupled-wave equations for the case of a cw pump, and he found that, for a sufficiently thin conjugator, an initially chirped pulse will be reflected with the opposite sense of chirp. He also showed that the output pulse is a rather complicated convolution of the input pulse if the conjugator is not sufficiently thin. Chirp reversal was subsequently discussed by Yariv, Fekete, and Pepper.[8] They considered the following situation: A short optical pulse upon passing through a dispersive material emerges temporally elongated and develops a linear chirp. If such a pulse is subsequently reflected by a sufficiently thin Kerr-like conjugator, chirp reversal will program the conjugate pulse so that upon its retraversal of the dispersive material, dispersive pulse compression will occur and the emerging pulse will be identical to the original pulse (i.e., in a double pass, dispersive spreading would cancel). In describing the conjugation of the chirped pulse, the authors presented a Fourier-transform relationship to which we shall devote the remainder of this paper.

Rigrod, Fisher, and Feldman[9] have developed an analytical time-domain expression for the delta-function response of a cw-pumped Kerr-like conjugator; it is a series of modified Bessel functions of integral order. For $\kappa l > \pi/2$, the solutions are unstable, in the sense that a finite input pulse results in a conjugate pulse of infinite energy and duration. Reference 9 relied upon an earlier analysis of active contraflow systems which Bobroff and Haus[10] had published over a decade ago. Opposite to the cw-pumped case we shall discuss, Miller[11] recently considered a conjugator with a transit time very much longer and with a pump pulse very much shorter than the probe pulse. In this interesting limit, the conjugator truly time reverses the probe envelope.

In this paper we develop the interrelationships between the steady-state behavior and the transient behavior for cw-pumped Kerr-like conjugators in which the optical Kerr effect is considered to respond instantaneously. We use standard linear techniques even though the original problem could be construed as a *nonlinear* one. We develop an *antilinear* fast-Fourier-transform technique that allows us to calculate rapidly the conjugate reflected wave form for input pulses of arbitrary form.[12] Phenomena associated with pulse reshaping, chirping, and chirp reversal are readily simulated.

Section II uses Laplace-transform techniques to show the general relationship between the transient and steady-state responses, and it demonstrates that for $\kappa l < \pi/2$, an *antilinear* Fourier-transform relationship exists. Section III shows the results of numerically applying this Fourier-transform technique to a number of pulse reshaping and chirp-related matters.

II. RELATIONSHIP BETWEEN TRANSIENT AND STEADY-STATE EFFECTS

A. General relationships

In this section we develop the fundamental relationships between the transient and the steady-state responses. We obtain antilinear relationships that will allow us to treat the problems numerically through relatively standard Fourier-transform techniques. As in Fig. 1, we consider an antireflection coated slab of transparent nonlinear dielectric material extending infinitely in the x and y directions, and extending in the z direction (x, y, z are Cartesian coordinates) from $z=0$ to l. The material is pumped by two equal-intensity counterpropagating plane waves of frequency ω_0. We assume throughout that these pumps are not depleted, that they remain plane waves in the medium, and that they are significantly stronger than the probe and conjugate waves. We assume that all waves are plane polarized in the same direction. A probe wave propagates towards the right and impinges on the dielectric at $z=0$. Its electric field E_p is represented as

$$E_p = \tfrac{1}{2}\mathcal{E}_p \exp[-i\omega_0(t - z/v)] + \text{c.c.} \tag{1}$$

A conjugate wave is generated within the dielectric and propagates toward the left; we represent its field E_c as

$$E_c = \tfrac{1}{2}\mathcal{E}_c \exp[-i\omega_0(t + z/v)] + \text{c.c.} \tag{2}$$

where $\mathcal{E}_c$ and $\mathcal{E}_p$ are assumed to be slowly varying functions of x, y, z, and t. Because of their low intensity, neither the conjugate nor the probe wave experiences self-focusing or self-phase

modulation. In Eqs. (1) and (2), v denotes the linear phase velocity of light in the dielectric. We do *not* require that the probe wave be exactly at the frequency of the pump. If E_p is centered on $\omega_0+\Delta$ then E_c will be centered on $\omega_0-\Delta$ and the envelopes $\mathcal{E}_p$ and $\mathcal{E}_c$ will carry, respectively, factors $\exp[-i\Delta(t-z/v)]$ and $\exp[+i\Delta(t+z/v)]$ in addition to other x, y, z, and t dependence. As long as $\Delta \ll \omega_0$, inclusion of these exponential factors will in no way affect the validity of the slowly varying amplitude approximation; we shall therefore assume that $\mathcal{E}_p$ and $\mathcal{E}_c$ vary slowly in t and in z as compared with the exponential factors in Eqs. (1) and (2). This results in the well-known[7,9,10] coupled set

$$\frac{\partial \mathcal{E}_p}{\partial z}+\frac{1}{v}\frac{\partial \mathcal{E}_p}{\partial t}=-i\kappa\mathcal{E}_c^*\,,$$
$$\frac{\partial \mathcal{E}_c^*}{\partial z}-\frac{1}{v}\frac{\partial \mathcal{E}_c^*}{\partial t}=-i\kappa^*\mathcal{E}_p\,, \tag{3}$$

where κ is the complex-coupling coefficient evaluated at $\omega=\omega_0$. The parameters v and κ are constants. Because $\mathcal{E}_c$ and $\mathcal{E}_p$ may depend weakly upon x and y, they need not be plane waves, but Eqs. (3) do neglect diffraction.

A known pulse of radiation is introduced as a probe and enters the medium at $z=0$. Thus at $z=0$ we have

$$\mathcal{E}_p(0,t)=F(t)\,, \tag{4}$$

where $F(t)$ is a prescribed function. The conjugate wave is generated in the medium, not introduced from the right; thus at $z=l$,

$$\mathcal{E}_c(l,t)=0\,. \tag{5}$$

Equations (3) plus the boundary conditions, Eqs. (4) and (5), completely specify our problem.

We shall solve by Laplace transforming in t. However, as we do not wish to require that $F(t)$ vanish for negative t, we must employ the two-sided[13] (rather than the normal) Laplace transform. We denote tranformed functions by lowercase letters; thus

$$e_p(z,s)=\frac{1}{\sqrt{2\pi}}\int_{-\infty}^{\infty}\mathcal{E}_p(z,t')e^{-i\gamma t}dt\,, \tag{6}$$

and so on. For our purposes, we can restrict our attention to probe pulses of finite total energy; $F(t)$ therefore belongs to L_2. We shall further require that $F(t)\to 0$ sufficiently rapidly as $t\to-\infty$ that the integral

$$\int_{-\infty}^{0}F(t)e^{-\gamma t}dt \tag{7}$$

converges for all positive γ. This is guaranteed, for example, if $F(t)$ decays ultimately as $\exp(-bt^2)$ as $t\to-\infty$. These restrictions on $F(t)$ guarantee that its (two-sided) transform $f(s)$ has no singularity for $\mathrm{Re}(s)\geq 0$.

Since we are interested in $\mathcal{E}_c(z,t)$, we take the complex conjugate of Eqs. (3) and Laplace transform the result, obtaining

$$\frac{de_p^*}{dz}+\left(\frac{s}{v}\right)e_p^*-i\kappa^*e_c=0\,,$$
$$\frac{de_c}{dz}-\left(\frac{s}{v}\right)e_c-i\kappa e_p^*=0\,. \tag{8}$$

Here the symbol $e_p^*(s)$ denotes the Laplace transform of the complex conjugate of $\mathcal{E}_p(z,t)$, *not* the complex conjugate of the transform. The general solution to Eq. (8) is

$$-i\kappa e_p^*=[(s/v)-i\beta]Ae^{i\beta z}+[(s/v)+i\beta]Be^{-i\beta z}\,,$$
$$e_c=Ae^{i\beta z}+Be^{-i\beta z}\,, \tag{9}$$
$$\beta=[|\kappa|^2-(s/v)^2]^{1/2}\,,$$

where A and B are constants which, so far, are arbitrary. Because our pumps are exactly counterpropagating plane waves of equal intensity. and because the medium is nonresonant, then κ may, without loss of generality, be taken to be real and positive. For the remainder of this paper we will discontinue absolute value bars about κ.

The Laplace transforms of boundary conditions (4) and (5) become

$$e_p^*(0,s)=f^*(s)\,,\quad e_c(l,s)=0\,, \tag{10}$$

and these determine the constants

$$A=(-i\kappa/D)e^{-i\beta l}f^*(s)\,,$$
$$B=(i\kappa/D)e^{i\beta l}f^*(s)\,, \tag{11}$$
$$D=-2i[\beta\cos\beta l+(s/v)\sin\beta l]\,.$$

The conjugate wave at depth z is given by the second of Eqs. (9). Inserting the above values of A and B the result may be written as

$$e_c(z,s)=h(z,s)f^*(s)\,,$$
$$h(z,s)=\frac{-i\kappa\sin[\beta(l-z)]}{\beta\cos\beta l+(s/v)\sin\beta l}\,, \tag{12}$$
$$\beta=[\kappa^2-(s/v)^2]^{1/2}\,.$$

Taking the inverse Laplace transform, we have

$$\mathcal{E}_c(z,t)=\frac{-i}{\sqrt{2\pi}}\int_{\gamma-i\infty}^{\gamma+i\infty}h(z,s)f^*(s)e^{st}ds\,, \tag{13}$$

where γ is subject, by causality, to the sole restriction that all singularities of the integrand lie to the left of the path of integration. Note that

$h(z,s)$ assumes the role of a transfer function. For $z=0$, $h(z,s)$ is formally identical to the *steady-state* filter function found by Bobroff,[14] and by Pepper and Abrams,[6] which means that, just as in linear optics, one can generate any *transient* behavior knowing only the steady-state responses at all frequencies. If one examines Eq. (13) for a temporal delta-function input [$F(t)=\delta(t)$, or $f(s)=1$], one readily obtains Eq. (38) of Ref. 10. In Appendix A we prove that for $F(t)=\delta(t)$ our Eq. (13) yields precisely the series of modified Bessel functions given as Eq. (3) in Ref. 9.

Note that in Eqs. (7)–(13) there is no reason why v and κ may not depend upon s, the complex frequency. This means that our technique applies both to Kerr-like conjugators in which the linear index of refraction varies with frequency and to conjugators that employ the saturable behavior of an absorbing or amplifying medium.[15] Appendix B discusses why v and κ cannot depend arbitrarily upon frequency. It also discusses the closely related limitations imposed by the slowly varying envelope approximation.

Since the line of integration in Eq. (13) must be to the right of all singularities of the integrand, we must know something about where these singularities lie. Our restrictions on $F(t)$ guarantee that $f(s)$ has no singularity on the imaginary axis nor in the right half-plane. Therefore only singularities of $h(z,s)$ need concern us, and these are discussed in detail in Appendix C. This appendix shows the following facts:

(1) The singularities are all poles.

(2) If $\kappa l<\pi/2$, all these poles lie to the left of the imaginary s axis.

(3) If, for some integer n, we have $(n-\frac{1}{2})\pi<\kappa l<(n+\frac{1}{2})\pi$, then there are exactly n poles in the right half-plane. These poles are all simple and they all lie on the real s axis.

Now let there be exactly n poles in the right half-plane and denote their location by $s=s_k$, $k=1,2,\ldots,n$. Let h_k denote the residue of $h(z,s)$ at $s=s_k$. A procedure for computing $\{s_k\}$ and $\{h_k\}$ is given in Appendix C. We now form the function $g(z,s)$, defined by

$$g(z,s)=h(z,s)-\sum_{k=1}^{n}\frac{h_k}{(s-s_k)}. \tag{14}$$

As the poles at $s=s_k$ are all simple, it follows that $g(z,s)$ has no poles in the right half-plane, and therefore we may set $\gamma=0$ in the integral over g. Thus if we solve Eq. (14) for $h(z,s)$ and set the result into Eq. (13), we obtain our central result, namely,

$$\mathcal{E}_c(z,t)=\frac{1}{\sqrt{2\pi}}\int_{-\infty}^{\infty}g(z,-i\Omega)f^*(-i\Omega)e^{-i\Omega t}d\Omega+\sum_{k=1}^{n}h_k f^*(s_k)e^{s_k t}. \tag{15}$$

Here $\Omega=-\operatorname{Im}(s)$.

B. Specialization to stable operation

The integral in Eq. (15) connects the input and the conjugate waves through an antilinear Fourier-transform relationship. Before discussing the integral, we wish for several reasons to restrict our interest to the case of stable operation, in which $\kappa l<\pi/2$. Our treatment of the unstable case is of limited validity because the exponential growth of the conjugate wave will eventually violate the condition that the conjugate wave be weaker than the pump wave, and also because the effect of spontaneous optical parametric emission is not taken into account. Such a quantum-mechanical effect can be thought of as the conjugate reflection of zero-point photons, a matter not at all considered in our classical starting equations. For the above reasons, we restrict our attention to the regime in which $\kappa l<\pi/2$. Clearly, $n=0$. The sum in Eq. (15) disappears, and $g(z,s)=h(z,s)$.

We shall denote the Fourier transform[16] of a function by a tilde, for example:

$$\tilde{\mathcal{E}}_p(\Omega)=\frac{1}{\sqrt{2\pi}}\int_{-\infty}^{\infty}\mathcal{E}_p(t')e^{i\Omega t'}dt'. \tag{16}$$

where $\Omega=\omega-\omega_0$. Accordingly, $f^*(-i\Omega)=\tilde{\mathcal{E}}_p^*(\Omega)=[\tilde{\mathcal{E}}_p(-\Omega)]^*$. We then write Eq. (15) in a form most amenable to numerical analysis:

$$\mathcal{E}_c(z,t)=\frac{1}{\sqrt{2\pi}}\int_{-\infty}^{\infty}h(z,-i\Omega)[\tilde{\mathcal{E}}_p(-\Omega)]^*e^{-i\Omega t}d\Omega. \tag{17}$$

This equation is our desired prescription for numerically computing the conjugate wave forms. First one Fourier transforms the input pulse, then one multiplies the antilinear transfer function h by the complex conjugate of the Fourier component at frequency $-\Omega$, and finally one inverse-Fourier-transforms to obtain the output wave form. The importance of this equation is that, for an arbitrary input pulse, one can readily apply standard fast-Fourier numerical techniques[17] first to obtain the function $[\tilde{\mathcal{E}}_p(-\Omega)]^*$ and subsequently to evaluate the integral in Eq. (17). The relationship derived here for stable operation is precisely that anticipated in Ref. 8. The Fourier transform of Eq. (17),

$$\tilde{\mathcal{E}}_c(z,\Omega) = h(z,-i\Omega)[\tilde{\mathcal{E}}_p(-\Omega)]^*, \quad (18)$$

shows that the spectrum of the conjugate wave at upshifted frequency Ω is equal to the antilinear transfer function times the complex conjugate of the input spectral component evaluated at the downshifted frequency $-\Omega$. This is precisely the cw relationship described by Eq. (6) of Ref. 6.

Note the difference between the above development and the more conventional *linear* optical system described by a transfer function $T(z,\Omega)$. The linear counterparts of Eqs. (17) and (18) contain, instead, the product $T(z,\Omega)\tilde{\mathcal{E}}_p(\Omega)$, which means that input at one frequency comes out at the same frequency. Note also that, in conventional linear optics, the complex-conjugation operation is missing.

The extension of our numerical procedure to unstable ($\kappa l \geq \pi/2$) operation is simple. First, one subtracts off the unstable poles as shown in Eq. (14). Next, one carries out the prescription as outlined for stable operation using $g(z,-i\Omega)$ in place of $h(z,-i\Omega)$. Finally, one adds back the contribution of the unstable poles given by Eq. (15).

III. NUMERICAL SIMULATIONS

A. Introduction

Section II describes a technique for rapidly calculating the conjugate wave forms for arbitrary input pulses. In this section we apply that technique to a number of interesting cases. In general our numerical calculations proceed as follows: First the possibly complex input-pulse envelope expression $\mathcal{E}_p(t)$ is evaluated on an appropriately chosen 4096-point uniform time grid. The fast-Fourier transform[17] is applied, and the resulting complex spectral function is point-by-point inverted about the pump-wave frequency. This new spectral function is then complex conjugated before multiplying by the appropriate antilinear transfer function. The resulting distribution is inverse-fast-Fourier transformed to obtain the conjugate wave form $\mathcal{E}_c(t)$.

Several functions are then readily calculated. The intensity versus time $|\mathcal{E}_c(t)|^2$ and the spectral intensity $|\tilde{\mathcal{E}}_c(\Omega)|^2$ are generated. The instantaneous phase perturbation $\delta\phi(t)$ is found by evaluating $\tan^{-1}[\mathrm{Im}\mathcal{E}_c(t)/\mathrm{Re}\mathcal{E}_c(t)]$ and by then piecewise fitting together the discontinuous function through addition or subtraction (where appropriate) of integral multiples of π. The instantaneous frequency shift $\delta\omega(t)$ is found by computing $-\partial(\delta\phi)/\partial t$.

The fast-Fourier transform cannot be used properly without certain precautions: The bandwidths of both the conjugator and the input pulse must lie well within the allotted spectral window. Any physical pulse must be defined on a sufficiently fine time grid that the temporal resolution is adequate. The temporal width of the input pulse must lie within the allotted time window. Problems associated with aliasing must be avoided, because an improperly chosen window will truncate the trailing edge of a pulse, and the truncated trailing edge will unfortunately modify the leading edge of the output pulse. The calculations which follow take all of these points into consideration.

B. The delta-function response

To simulate the temporal delta function, we set $\mathcal{E}=0$ at all but one temporal point. We thus are replacing the delta function with a triangular pulse whose half-width equals the temporal step size. For $\kappa l=\pi/4$, the calculated conjugate wave form is shown as the dashed line in Fig. 2. For comparison purposes, the solid line in Fig. 2 is the corresponding closed-form analytic expression previously published in Ref. 9 and derived here as Eq. (A23). The vertical separation between the two curves is introduced for comparison purposes only; the curves are virtually identical. The conditions associated with Fig. 2 are $l=6.6$ cm, $n=1.62$, and $\kappa l=\pi/4$.

Figure 2 shows that for a delta-function input the results of the antilinear Fourier-transform technique are in excellent agreement with the analytical answer for over ten orders of magnitude in intensity. This agreement is especially encouraging because the calculated delta-function response is a very critical test of any numerical technique. The calculated delta-function response exhibits many interesting features. Obviously, there is no response until the time the delta-function pulse strikes the entrance face of the conjugator. At that time the conjugate signal rises abruptly and thereafter it gradually rises until the round-trip time of the conjugator. At that first round-trip time, the conjugate signal drops abruptly to a lower value and thereafter rapidly approaches exponential decay. The explanation for the gentle rise during the first round-trip transit time is simple: As the delta-function pulse passes through the conjugator it generates a backward conjugate wave. Because of the narrow-band reflectivity of the conjugator, the backward wave spectrum is peaked at the pump-wave frequency of the conjugator, in contrast to the flat spectrum associated with the forward-traveling delta function. As the backward wave travels through the conjugator on its way out, it too gets conjugated into a forward-going wave. This conjugation and reconjugation continuously couples

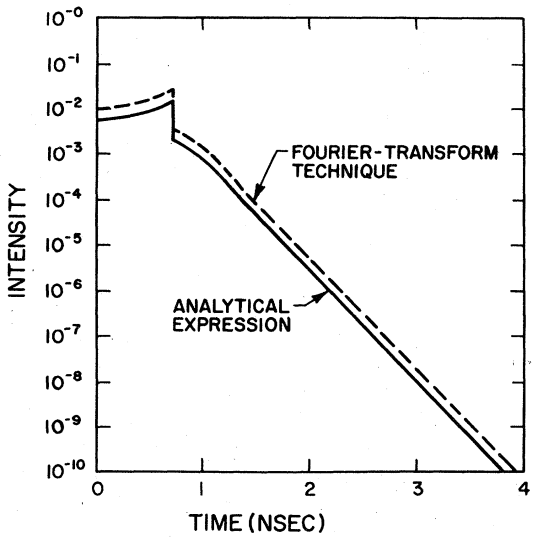

FIG. 2. The calculated delta-function response. The dashed line shows the result of the calculations using the Fourier-transform techniques presented in this paper. For comparison, the solid line was calculated from the analytical expression in terms of the series of modified Bessel functions (taken from Eq. A23). The artificial vertical separation between the two curves is for comparison purposes only. The conditions for this calculation are $l = 6.6$ cm, $n = 1.62$, $\kappa l = \pi/4$.

forward- and backward-going waves and it puts a smooth tail on the forward-going delta function. It is the growth of this smooth tail which accounts for the increase in conjugate intensity as the delta-function pulse is traversing the device.

As the delta-function pulse leaves the conjugator, only the temporally smooth backward- and forward-going waves remain inside; the delta function no longer is generating a "new" backward wave. This accounts for the sudden discontinuous decrease in the conjugate signal at the time that an observer at the entrance face could first learn that the delta function has left the sample. Because $\kappa l < \pi/2$, the coupling is inadequate for the remaining waves subsequently to generate stronger partial waves and, therefore, the waves (both forward and backward) rapidly approach an exponential decay.

For $\kappa l \ll 1$, the delta-function response is merely a flat-topped function that turns on at $t = 0$ and turns off at the round-trip transit time. This also can be easily understood in the partial-wave picture; the coupling is so weak that the primary backward-going wave is not reconjugated and, therefore, no tail grows on the forward-going delta function. Thus the radiated intensity is constant until the round-trip transit time, and thereafter the output is zero because the reconjugation of the partial waves can be neglected. This point was clearly appreciated by Marburger.[7]

As κl is increased to $\pi/2$, the exponential decay becomes a slower and slower process. With proper precautions to avoid aliasing, our numerical calculation of the delta-function response is in excellent agreement with the analytical expression for values of κl as high as 1.5. If we try the inverse-Fourier transform of the transfer function for κl slightly larger than $\pi/2$, namely, 1.6, we get a clearly incorrect answer. This is to be expected because of the appearance of a pole in the right-hand half-plane. To continue using the Fourier-transform techniques for values of κl above or equal to $\pi/2$, we would have to treat the transfer function g [as described in Eq. (14)], and then to account separately for each pole which had crossed into the right half-plane [as outlined in Eq. (15)]. Clearly, this same technique can be applied to cases in which κl is only slightly less than $\pi/2$. The pole, although still in the left-hand plane, can be separately accounted for. This procedure could greatly ease aliasing problems.

C. Temporal spreading in conjugate reflection

As was shown in the previous section, a temporal delta function is converted into a conjugate pulse with a duration longer than the round-trip transit time of the conjugator. To examine the influence of this type of temporal spreading, we performed a series of calculations. A $\frac{1}{2}$-nanosecond (FW$\frac{1}{e}$M) duration temporally Gaussian pulse is conjugated by an infrared-pumped germanium conjugator ($n = 4$). To examine the role of pulse spreading, we have considered various conjugators, with $\kappa l = \pi/4$, but with l (and, correspondingly, κ) variable. Thus the conjugate reflectivity *on resonance* is unity, but the effective bandwidth of the conjugator is varied.

Figure 3 shows the results of the calculation. The input pulse (with carrier frequency chosen equal to the pump-wave frequency) is shown for comparison purposes. Note the decrease in peak intensity and the increase in temporal duration as the physical thickness of the conjugator is varied from 1 to 5 cm. These results can be explained noting that the induced gratings consist of more and more lines as the conjugator becomes longer. Hence, the bandwidth of the conjugator is reduced to such an extent that it cannot efficiently conjugate all the frequency components in the input pulse. The results of Fig. 3 are recast in Fig. 4. Peak intensity and total energy were evaluated for each conjugate wave form. Both quantities are plotted as functions of the ratio of the conjugator round-trip transit time to the duration of the

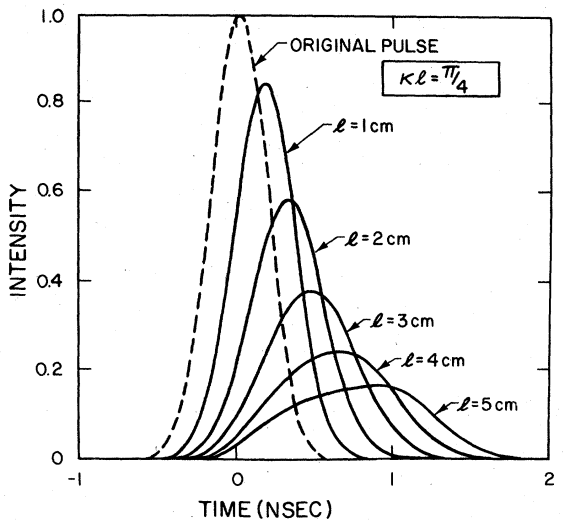

FIG. 3. Temporal spreading of the conjugate pulse. This calculation was performed by keeping κl equal to $\pi/4$ (so that the conjugate reflectivity on resonance is unity), but with l (and, correspondingly, κ) variable. This procedure varies the effective bandwidth of the conjugator. The original pulse (0.5 nsec FW$\frac{1}{e}$M) is shown by the dashed line. The conjugator material is germanium with a refractive index of 4.0.

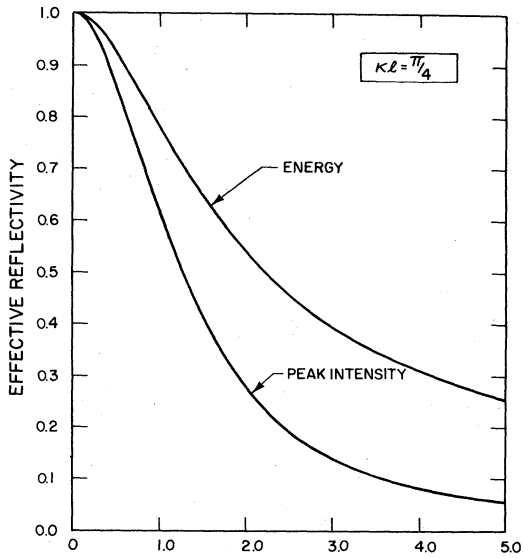

FIG. 4. The calculated degradation in effective reflectivity when the probe-pulse duration becomes shorter than the thickness of the conjugator. Plotted are both the integrated conjugate energy and the intensity at the peak of the conjugate pulse. All other conditions are the same as in Fig. 3.

pulse. Note that the intensity curve falls off much faster than the energy curve, a manifestation of the temporal broadening process. In summary, the results obtained indicate that even if a conjugator has a cw reflectivity of unity, the practical reflectivity will be greatly reduced unless the duration of the input pulse is far longer than the round-trip transit time of the conjugator.

D. Chirp reversal

For a broadband conjugator, the implications for chirp reversal are clear; if $h(z, -i\Omega)$ is set to be constant in Eq. (17), the chirp (rate of change of instantaneous frequency with time) of the conjugate pulse is precisely opposite to that of the input pulse. This fact was first pointed out by Marburger.[7] Yariv, Fekete, and Pepper[8] showed that a pulse that had undergone dispersive spreading would be conjugated in a suitable broadband conjugator so that the chirp reversal would cause subsequent dispersive narrowing upon retraversal of the dispersive element. Our calculations verify this, but, more importantly, they can be used to evaluate the degradation in chirp reversal when the bandwidth of the conjugator is inadequate.

We have analyzed the degree of chirp reversal under the conditions discussed in Sec. III C. Again, the conjugate reflectivity was set equal to unity on resonance, and the physical thickness of the germanium conjugator was varied (as an adjustment of its bandwidth). The same temporally Gaussian probe pulse was used, but this time it had impressed upon it a positive linear chirp of such a magnitude that the bandwidth is twice that of an unmodulated pulse. At the peak of the input pulse, the instantaneous frequency is that of the pump waves.

Figure 5 shows the results of that calculation. The instantaneous frequency shift is plotted as a function of time for both the input pulse and for the conjugate pulses, with conjugator thicknesses of 0.1, 1.0, and 2.0 cm. As in the previous figures, $t = 0$ is the time at which the peak of the probe pulse strikes the input face of the conjugator. Note that for the thinnest conjugator ($l = 0.1$ cm), the bandwidth of the device is adequate to produce nearly perfect chirp reversal, but that for greater thicknesses the chirp reversal is incomplete. The chirp shows a rather distinct diminution (as evidenced by a flattening of the frequency-versus-time curves) at approximately the time that the conjugate pulse peaks. Thus we see that a chirped pulse is conjugated as a relatively chirp-free pulse in this narrow-bandwidth limit.

In a related calculation, κl was set equal to $\pi/4$, and the conjugator thickness was set equal to 2 cm,

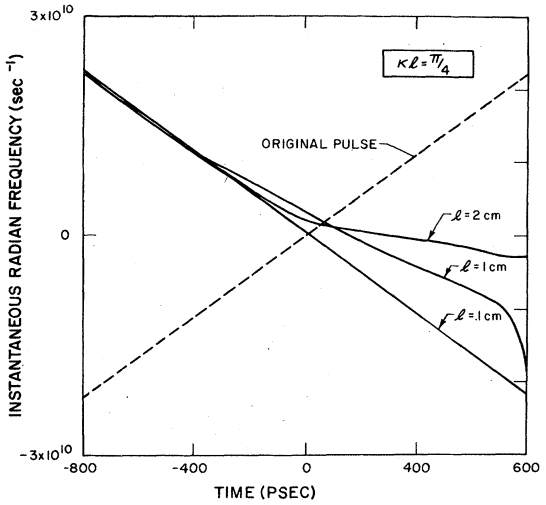

FIG. 5. Study of the chirp-reversal process. The instantaneous frequency shift versus time is shown for the positively chirped input pulse. Again (as in the previous two figures) the cw on-resonance conjugate reflectivity is unity but the physical thickness of the conjugator is varied. Note that for physically thin conjugator (i.e., one that is sufficiently broadband), the chirp reversal is nearly perfect, but that for thicker conjugators, the chirp at the peak of the pulse is significantly reduced.

and the chirp was varied. We found that increasing the chirp on the input pulse resulted in decreasing the duration of the conjugate pulse. This can be easily understood by considering that as the chirp becomes more severe, the pulse sweeps more quickly through the high-reflectivity center frequency of the conjugator.

To study the chirp degradation by weaker conjugators, we repeated the above calculations with much smaller values of κl. As anticipated, we find that the chirp modification at fixed l does not tend towards perfect chirp reversal, but, instead becomes asymptotically independent of the value of κl. This tendency can be understood as follows: As one decreases κl, the delta-function response becomes a flat-topped function for the round-trip duration of the conjugator. The duration of the function depends only upon l, and the height of the function depends only upon κ. Thus the inverse-Fourier transform of this limiting function has a spectral width that depends only upon l, as clearly shown in Eq. (8) of Ref. 6. This inability of a physically thick conjugator (in the weak coupling limit) to reverse the input-pulse chirp was first noted by Marburger,[7] and it can easily be understood in terms of the impressed gratings; the resolution is merely determined by the number of lines in the gratings.

All calculations in this section were repeated with equivalent negatively chirped pulses, and the curves obtained are just right-left mirror images of the originally calculated curves. Thus our chirp-reversal conclusions apply to input pulses with either positive or negative chirp. Pepper and Yariv have recently shown[18] that a conjugator with a reflectivity of unity will compensate for the interposition of a weakly nonlinear aberrator as long as catastrophic self-focusing does not occur. Clearly, considerations of this section would require the transit time of the conjugator to be far less than the duration of the input pulse. Otherwise the time-varying divergence [which is equivalent to a spatially (x, y) dependent chirp] would not be faithfully reversed.

E. The inverse problem

One can ask the inverse question: To obtain a desired conjugate wave form, what probe pulse is needed? The transfer function appropriate to this question is merely $[h(z,s)]^{-1}$, which, unfortunately, is not as well behaved as is $h(z,s)$. This inverse problem will be discussed in a later paper.

IV. CONCLUSIONS

We have used linear techniques to develop a powerful and rapid numerical method for computing the transient response of a cw-pumped Kerr-like four-wave mixing conjugator. Our algorithm is based on expressing the conjugate response in terms of an antilinear Fourier transform, with, in the unstable case, correction terms. A complete derivation is presented, along with a comparison of these results to others in the literature.

Our numerical examples clearly show that a conjugator whose round-trip transit time is comparable to the duration of the input pulse will very noticeably broaden and delay the conjugate reflection. This effect is consistent with the narrow-band nature of the cw filter function. We have also calculated examples that show the effect of conjugator length upon the quality of chirp reversal: The longer the conjugator (the narrower its bandwidth) the greater the departure of the conjugate pulse from complete chirp reversal. As our examples show, the leading edge of the conjugate pulse shows most faithful chirp reversal, and the peak of the conjugate pulse exhibits the largest deviation from faithful chirp reversal. This also indicates that too long a conjugator will be unable to correct for the onset of self-focusing in a mildly nonlinear distorter.

Note added. We have recently become aware of a letter by B. Ya. Zel'dovich, M. A. Orlova, and

V. V. Shkunov (Dok. Akad. Nauk SSSR 252, 595 (1980) [Sov. Phys—Dokl. 25, 390 (1980)]). Their Eqs. (3) correspond to our Eqs. (12), and their Eq. (8) gives the leading term of our Eq. (A23).

ACKNOWLEDGMENTS

We are grateful to J. F. Figueira for support and encouragement and to W. W. Rigrod for numerous helpful suggestions. This work was performed under the auspices of the U. S. Department of Energy.

APPENDIX A: INVERSE LAPLACE TRANSFORM FOR A DELTA-FUNCTION INPUT

By evaluating the Laplace transform of the antilinear transfer function, we obtain for unrestricted κl, the conjugate response to a delta-function input. Our result will agree with the modified Bessel function series given in Refs. 9 and 10. This agreement offers further proof of the correctness of our approach. To simplify the notation, we normalize our input, setting $F(t) = (-i\kappa)^{-1}\delta(t)$. Then $f(is) = (-i\kappa\sqrt{2\pi})^{-1}$, and our problem is to evaluate the Laplace transform:

$$\bar{H}(t) = \frac{1}{2\pi i}\int_{\gamma-i\infty}^{\gamma+i\infty} \bar{h}(s)e^{st}ds\,,$$

$$\bar{h}(s) = \frac{\sin\beta l}{\beta\cos\beta l + (s/v)\sin\beta l}, \qquad \text{(A1)}$$

$$\beta = [\kappa^2 - (s/v)^2]^{1/2}.$$

The bars over H and h indicate their normalization by the factor of $(-i\kappa)^{-1}$ and indicate that the functions are evaluated at $z = 0$.

For convenience, let us write

$$a = v\kappa\,, \quad \tau = 2l/v\,, \qquad \text{(A2)}$$
$$\alpha = iv\beta = (s^2 - a^2)^{1/2}.$$

Note that τ is the round-trip transit time. We now replace the trigonometric functions by their expressions in terms of exponentials, so that

$$\bar{h}(s) = \bar{h}_1(s) + \bar{h}_2(s) = v\phi(s) - ve^{-\alpha\tau}\phi(s)\,, \qquad \text{(A3)}$$

$$\phi(s) = [(s+\alpha) - (s-\alpha)e^{-\alpha\tau}]^{-1}.$$

We can apply the contour integral theorem separately to the two terms $\bar{h}_1(s)$ and $\bar{h}_2(s)$, to find that (i) $\bar{H}_1(t)$ turns on at $t = 0$, just as the probe pulse enters the medium, and (ii) $\bar{H}_2(t)$ turns at $t = \tau$, i.e., when an observer at $z = 0$ could first learn that the delta-function pulse has left the medium at $z = l$.

We shall follow the procedure outlined in Ref. 10 to evaluate the transform using contour integration. Of course, the end result will apply for all times, including the initial transit period. Starting with Eq. (A3) for $\bar{h}(s)$, we formally expand $\phi(s)$ in a power series in $X[\exp(-\alpha\tau)]$, where

$$X = \frac{s-\alpha}{s+\alpha} = \frac{a^2}{(s+\alpha)^2}\,, \qquad \text{(A4)}$$

obtaining the series

$$\bar{h}(s) = \frac{v}{s+\alpha} - 2v\sum_{n=1}^{\infty}\frac{\alpha a^{2(n-1)}}{(s+\alpha)^{2n}}e^{-n\alpha\tau}. \qquad \text{(A5)}$$

This expansion is suggested by Ref. 10. First we shall show that this series is uniformly convergent for $s = \nu - i\Omega$, $\nu > a$, and all Ω. This will allow us to Laplace transform term by term.

Let us write

$$s = \nu - i\Omega, \quad \alpha = \rho e^{i\theta}. \qquad \text{(A6)}$$

Our expansion has introduced branch points at $s = \pm a$. If we are to integrate term by term, the line of integration must lie to the right of these new branch points; thus, we shall require

$$\nu > a\,. \qquad \text{(A7)}$$

Now, from Eq. (A6) we have

$$\rho^4 = (\nu^2 - \Omega^2 - a^2)^2 + 4\nu^2\Omega^2\,,$$
$$\tan 2\theta = \frac{-2\nu\Omega}{\nu^2 - a^2 - \Omega^2}\,. \qquad \text{(A8)}$$

From Eqs. (A7) and (A8) we see that as Ω increases from $-\infty$ to ∞, θ increases monotonically from $-\pi/2$ to $\pi/2$. Thus, $\mathrm{Re}(\alpha) > 0$ for all Ω and

$$\exp(-\alpha\tau) < 1\,. \qquad \text{(A9)}$$

Next, note that

$$|X|^2 = a^2/|s+\alpha|^2\,, \qquad \text{(A10)}$$

but

$$|s+\alpha|^2 = (\nu + \rho\cos\theta)^2 + (\Omega - \rho\sin\theta)^2\,. \qquad \text{(A11)}$$

As $\cos\theta$ is always positive, we see that

$$|s+\alpha|^2 > \nu^2 > a^2\,. \qquad \text{(A12)}$$

Thus, the series of Eq. (A5) converges uniformly over the whole line of integration and can be transformed term by term.

Consider, therefore, the Laplace transform of the nth term of the series Eq. (A10), namely,

$$L_n(t) = \frac{1}{2\pi i}\int_{\gamma-i\infty}^{\gamma+i\infty}\frac{\alpha a^{2n-2}}{(s+\alpha)^{2n}}\exp(st - n\tau\alpha)ds\,. \qquad \text{(A13)}$$

On the large circle $|s| = R \gg a$, we have $\alpha = s$. Thus we can always complete the contour for L_n; we complete to the right if $t < n\tau$ and to the left if $t > n\tau$. In the latter case we encircle all the singu-

larities, namely, the branch points $s = \pm a$. Clearly, $L_n(t) = 0$ for $t < n\tau$.

The trick in evaluating the integral of Eq. (A13) is to remove the branch points by a substitution[19] of the type $s = au + b/u$ and to integrate in the u plane. Trying this we readily see that the appropriate substitution is

$$s = \frac{ia}{2}\left[\left(\frac{t+n\tau}{t-n\tau}\right)^{1/2} u - \left(\frac{t+n\tau}{t-n\tau}\right)^{-1/2} u^{-1}\right]. \tag{A14}$$

With this change of integration variable, Eq. (A18) becomes

$$L_n(t) = -\frac{(-1)^n}{8\pi i}\left(\frac{t-n\tau}{t+n\tau}\right)^n \int_C \left[2u^{-2n-1} + \left(\frac{t-n\tau}{t+n\tau}\right)u^{-2n-3} + \left(\frac{t+n\tau}{t-n\tau}\right)u^{-2n+1}\right] \times \exp\left[\left(\frac{ia}{2}\right)(t^2 - n^2\tau^2)^{1/2}(u - u^{-1})\right] du, \tag{A15}$$

where C is a contour in the u plane which encloses the singularity at $u = 0$ once counterclockwise. Now recall the definition of the Bessel function, namely,[20]

$$J_n(x) = \frac{1}{2\pi i}\int_C u^{-n-1}\exp\left[\left(\frac{x}{2}\right)(u - u^{-1})\right] du. \tag{A16}$$

The contour in Eq. (A21) is exactly the same as in Eq. (A20); thus, using

$$J_n(ix) = i^n I_n(x) \tag{A17}$$

we get

$$L_n(t) = \frac{1}{4}\left[\left(\frac{t-n\tau}{t+n\tau}\right)^{n-1} I_{2n-2}(a(t^2 - n^2\tau^2)^{1/2}) - 2\left(\frac{t-n\tau}{t+n\tau}\right)^n I_{2n}(a(t^2 - n^2\tau^2)^{1/2}) + \left(\frac{t-n\tau}{t+n\tau}\right)^{n+1} I_{2n+2}(a(t^2 - n^2\tau^2)^{1/2})\right] S(t - n\tau). \tag{A18}$$

We have introduced the step function $S(t) = 0$ for $t < 0$ and $S(t) = 1$ for $t > 0$ to remind us that $L(t)$ vanishes for $t < n\tau$.

We have now transformed every term of Eq. (A5) except the first, namely,

$$L_0(t) = \frac{1}{2\pi i}\int_{\gamma - i\infty}^{\gamma + i\infty} (s + \alpha)^{-1} e^{st}\, ds. \tag{A19}$$

Clearly, this term turns on at $t = 0$. For $t > 0$, we proceed exactly as for L_n, setting

$$s = (ia/2)(u - u^{-1}), \tag{A20}$$

which, incidentally, is Eq. (A18) with $n = 0$. Then

$$L_0(t) = \frac{1}{4\pi i}\int_C (u^{-1} + u^{-3})\exp[(iat/2)(u - u^{-1})]\, du, \tag{A21}$$

and finally

$$L_0(t) = \tfrac{1}{2}[I_0(at) - I_2(at)]\, S(t) = (1/at) I_1(at) S(t). \tag{A22}$$

For the full evaluation of Eq. (A1) we therefore have

$$\bar{H}(t) = vL_0(t) - 2v\sum_{n=1}^{\infty} L_n(t), \tag{A23}$$

with L_0, L_n given by Eqs. (A22) and (A23). Thus we have evaluated the inverse transform by series expansion coupled with contour integration methods to find the impulse response given by Refs. 9 and 10 in the special case that the probe is introduced at $z = 0$ and that the conjugate return is observed at the same point. This series had previously been deduced by the method of images rather than by our present expansion of the integral. Note that, because of the step functions $S(t - n\tau)$, the series Eq. (A23) is actually finite for all finite t. Thus the delta-function response has been evaluated in closed form.

APPENDIX B: COMMENTS ON HIGH-FREQUENCY BEHAVIOR AND ON THE SLOWLY VARYING ENVELOPE APPROXIMATION

Equations (3) are derived from Maxwell's equations by making the slowly varying envelope approximation, and hence are valid only as long as s, the complex frequency of modulation of the envelope, is very small compared with the carrier frequency ω_0. In spite of this, Eq. (13) expresses our solution as an integration over an infinite range of s, or more precisely, if we set $s = \nu - i\Omega$, over an infinite range of Ω. Obviously this is a good approximation only if we restrict our attention to signals whose power spectra are confined to the immediate vicinity of ω_0. But this infinite range of integration contains a hidden caveat: if we generalize by allowing κ to depend on Ω we should be careful that $h(z, -i\Omega)$ remains quadratically integrable.

In their study of the steady-state response, Pepper and Abrams[6] found a frequency dependence of the coupling constant of the form $\kappa \propto (\omega_0 + \Omega)$. As they explicitly restrict the frequency range so

that $\Omega \ll \omega_0$, such a frequency dependence makes good sense in their problem. We, however, must be cautious of using such a frequency dependence of κ in Eq. (13) because it is not correct when $|\Omega| \to \infty$.

The frequency dependence found by Pepper and Abrams raises a related question. If we choose a cw monochromatic probe, specifying that

$$F(t) = \mathcal{E}_p(0,t) = \tfrac{1}{2} A \exp[-i\Omega(t - z/v)] + \text{c.c.}, \tag{B1}$$

then we are solving exactly the same problem as did Ref. 6. However, Ref. 6 finds $\kappa \propto (\omega_0 + \Omega)$ whereas we find $\kappa =$ constant. Which of us is right? Strictly speaking, neither. Both of us mutilate Maxwell's equations, because in making the slowly varying envelope approximation we ignore terms of order Ω/ω_0; but these two results differ precisely by a term of order Ω/ω_0. Therefore, insofar as the slowly varying envelope approximation is valid, the two different rules must be considered as being indistinguishable. Note, however, that our numerical method always uses a mesh so coarse that the condition $\Omega \ll \omega_0$ is effectively enforced. Thus, using either dependence causes us no computational difficulty. As a practical test of this last statement, all numerical examples of Sec. III were computed both ways. In all cases, the two results were indistinguishable.

Clearly, the delta-function response we calculate is the true transient response for the first-order set of coupled differential equations, but it is not correct for the more precise second-order set. Thus, our delta-function response should be considered only as a kernel for treating the conjugate reflection of input pulses which do not violate the slowing varying envelope condition.

APPENDIX C: SINGULARITIES OF $h(z,s)$

We will study the singularities of $h(z,s)$. We start with the prescription outlined in Ref. 10. Although β has branch points at $s = \pm v\kappa$, $h(z,s)$ has no such branch points because it is an even function of β. Therefore the only singularities of $h(z,s)$ are poles and they are the roots of the equation

$$\Delta = \beta l \cos\beta l + (sl/v)\sin\beta l = 0, \tag{C1}$$

Of these zeros, the one at $\beta = 0$ ($s = \pm v\kappa$) is not a pole because the numerator vanishes when $\beta = 0$.

It is convenient to write

$$Z = \beta l = [\kappa^2 - (s/v)^2]^{1/2}. \tag{C2}$$

Equation (C1) can then be rewritten as

$$(l/v)\sin Z/Z = -(\cos Z)/s = k, \tag{C3}$$

where k simply denotes the common value of the two expressions. We now use Eq. (C2) to determine k. Equations (C3) give

$$s^2 = (1/k^2)(1 - \sin^2 Z) = (1/k^2)[1 - k^2 Z^2 (v/l)^2]. \tag{C4}$$

Setting Eq. (C2) for Z into the extreme right-hand member of Eq. (C4), we see that the equation is satisfied if and only if we choose $k = \pm 1/(v\kappa)$. Thus Eqs. (C3) become

$$\sin Z = \pm Z/\kappa l, \qquad s = \mp v\kappa \cos Z. \tag{C5}$$

These equations are equivalent to Eq. (C1). As s and Z will in general be complex, we break Eqs. (C5) into real and imaginary parts, writing

$$s = \nu - i\Omega, \qquad Z = X + iY. \tag{C6}$$

Then the two complex Eqs. (C5) are replaced by four real equations, namely,

$$\begin{aligned} &\cos X \sinh Y = \pm Y/\kappa l, \\ &\sin X \cosh Y = \pm X/\kappa l, \\ &\nu = \mp \kappa v \cos X \cosh Y, \\ &\Omega = \mp \kappa v \sin X \sinh Y. \end{aligned} \tag{C7}$$

In these equations we must use all upper signs together and all lower signs together. At this point we depart from Ref. (10).

We have two classes of roots depending on whether $Y \neq 0$ or $Y = 0$. We now discuss these in turn.

Class A roots, $Y \neq 0$. When $Y \neq 0$ we can solve the first of Eqs. (C7) for $\cos X$ and set the result into the third. We get

$$\nu = -(v/l) Y \cosh Y/\sinh Y. \tag{C8}$$

As $Y\cosh Y/\sinh Y > 1$ for all $Y \neq 0$, we see that

$$\nu < -v/l \tag{C9}$$

for all class A roots. Thus, all class A roots lie in the negative half s plane and are well bounded away from the imaginary s axis. The first two of Eqs. (C7) are indifferent to the algebraic signs of X and Y. Thus, the replacement $X \to -X$ or $Y \to -Y$ simply changes the sign of Ω. Generally, the class A roots form an infinite set which occur in complex conjugate pairs.

If $\kappa l < 1$, there will be one real class A root. For $\Omega = 0$ we need $X = 0$ and we have

$$\sinh Y = Y/\kappa l, \qquad \nu = -\kappa v \cosh Y, \tag{C10}$$

for this root. If we set

$$\kappa l = 1 - \epsilon \tag{C11}$$

we find, for small ϵ,

$$Y^2 = 6\epsilon\,, \quad \nu = -(v/l)(1+2\epsilon)\,. \tag{C12}$$

Thus, as κl increases towards unity, this real root moves to the right towards the point $\nu = -(v/l)$, and $Y \to 0$. At $\kappa l = 1$, $Y = 0$ and this root changes class, becoming a class B root.

Class B roots, defined by $Y = 0$. Equation (C7) reduces to

$$\begin{aligned} &\sin X = \pm X/\kappa l\,, \\ &\nu = \mp \kappa v \cos X\,, \\ &\Omega = 0\,, \end{aligned} \tag{C13}$$

so these roots are all real, and can occur only if $\kappa l \geq 1$. If we set $\kappa l = 1 + \epsilon$, with ϵ small, we have

$$X^2 = 6\epsilon\,, \quad \nu = -(v/l)(1-2\epsilon)\,. \tag{C14}$$

Clearly, this is the real class A root which crossed the point $s = -v/l$ when κl went through unity. As κl continues to increase beyond unity, this root continues to move towards the right and crosses into the right half plane when κl reaches the value $\pi/2$.

Now let κl continue to increase beyond $\pi/2$. The above root moves farther into the right half plane, and the class A roots (now all complex) move towards the real axis. When κl reaches such a value that the equations

$$\cos X = \sin X/X = \pm 1/\kappa l \tag{C15}$$

are satisfied, two class A roots reach the point $s = -v/l$ and coalesce into a double class B root. As κl increases beyond this critical value, these two roots again split, one traveling to the right and the other to the left along the real s axis. They both remain class B roots. [It is clear that Eq. (C15) implies $Y = 0$.] This coalescing of class A roots happens first for $X = 4.493\,41$, $\kappa l = 1.465\,28\pi$. When κl reaches 1.5π the right-traveling root crosses into the right half plane. Next, when $X = 7.725\,25$, $\kappa l = 2.479\,50\pi$, two new class A roots coalesce into a double class B root which again splits. The right-traveling member crosses into the right half plane when $\kappa l = 2.5\pi$, and so on. We see, therefore, that if for some integer n,

$$(n - \tfrac{1}{2})\pi < \kappa l < (n + \tfrac{1}{2})\pi\,, \tag{C16}$$

there are exactly n poles in the right half plane.

We shall now show by direct calculation that all the class B poles

$$s = s_k = \nu_k \tag{C17}$$

are simple, provided $\nu_k \neq -v/l$. This calculation will provide a formula for finding the residue h_k of $h(z,s)$ at s_k,

$$h_k = \lim_{s \to s_k} [(s - s_k)h(z,s)]\,. \tag{C18}$$

Let us set

$$s = s_k + \epsilon \tag{C19}$$

and suppose ϵ to be small. Clearly, to first order in ϵ,

$$\begin{aligned} X &= l[\kappa^2 - (s_k + \epsilon)^2/v^2]^{1/2} \\ &= X_k - (l/v)^2 s_k \epsilon / X_k\,, \end{aligned} \tag{C20}$$

where X_k is X evaluated at $s = s_k$. Now set Eq. (C20) into Eq. (C1) (note $X = \beta l$). Expanding to lowest order in ϵ and remembering that $\Delta(s_k) = 0$, we get

$$\Delta = (\epsilon l/v)[1 + (l/v)\nu_k][\sin X_k - (l/v)\nu_k \cos X_k/X_k]\,. \tag{C21}$$

Because X_k, ν_k satisfy Eqs. (C13) this can be simplified. From Eqs. (C13) we have

$$-(l/v)\nu_k \cos X_k/X_k = \pm\,(\kappa l/X_k)\cos^2 X_k = \cos^2 X_k/\sin X_k\,, \tag{C22}$$

whence

$$\Delta = (\epsilon l/v)[1 + (l/v)\nu_k]/\sin X_k\,. \tag{C23}$$

It then follows that near the pole at $s = s_k$ we have

$$\begin{aligned} h(z,s) = &- i\kappa v \sin X_k \sin[X_k(1 - z/l)] \\ &\times \{(s - s_k)[1 + (l/v)s_k]\}^{-1}\,. \end{aligned} \tag{C24}$$

The poles at $s = s_k$ are therefore simple, provided $s_k \neq -v/l$, and the residues h_k are given by

$$\begin{aligned} h_k = &- i\kappa v \sin X_k [\sin X_k (1 - z/l)] \\ &\times [1 + (l/v)s_k]^{-1}\,, \\ X_k = &\, l[\kappa^2 - (s_k/v)^2]^{1/2}\,. \end{aligned} \tag{C25}$$

Everything is now spelled out. The class A poles are all well bounded away from and to the left of the imaginary s axis and hence are of no concern. If $\kappa l < \pi/2$ there are no poles in the right half plane and therefore no residues to evaluate. If condition (C16) is satisfied for some integer $n > 0$, then we must locate the n poles in the right half plane. This is most conveniently done by numerically solving the first of Eqs. (C13). Next one calculates $s_k = \nu_k$ from the second of Eqs. (C13). Once the set $\{s_k\}$ is determined one can readily calculate the set $\{h_k\}$ from Eq. (C25).

[1]See, for example, references cited in E. V. Ivakin, A. M. Lazaruk, and B. I. Stepanov, IEEE J. Quantum Electron. QE-15, 523 (1979) and cited in A. Yariv, *ibid.* QE-15, 524 (1979).
[2]R. W. Hellwarth, JOSA 67, 1 (1977).
[3]D. M. Bloom and G. C. Bjorklund, Appl. Phys. Lett. 31, 592 (1977).
[4]A. Yariv and D. M. Pepper, Opt. Lett. 1, 16 (1977).
[5]See references cited in A. Yariv, IEEE J. Quantum Electron. QE-14, 650 (1978).
[6]D. M. Pepper and R. L. Abrams, Opt. Lett. 3, 212 (1978).
[7]J. H. Marburger, Appl. Phys. Lett. 32, 372 (1978).
[8]A. Yariv, D. Fekete, and D. M. Pepper, Opt. Lett. 4, 52 (1979).
[9]W. W. Rigrod, R. A. Fisher, and B. J. Feldman, Opt. Lett. 5, 105 (1980).
[10]D. L. Bobroff and H. A. Haus, J. Appl. Phys. 38, 390 (1967).
[11]D. A. B. Miller, Opt. Lett. 8, 300 (1980).
[12]A preliminary version of this work was presented as Talk E.8 at the Eleventh International Quantum Electronics Conference, Boston, June, 1980 (unpublished). The abstract of this talk appeared as R. A. Fisher, B. R. Suydam, W. W. Rigrod, and B. J. Feldman, JOSA 70, 602 (1980).
[13]G. Doetsch, *Theorie und Anwendung der Laplace-Transformation* (Dover, New York, 1943), pp. 32,33, and 104.
[14]D. L. Bobroff, J. Appl. Phys. 36, 1970 (1965).
[15]T. Y. Fu and M. Sargent III, Opt. Lett. 4, 366 (1979).
[16]See, for example, J. M. Stone, *Radiation and Optics* (McGraw-Hill, New York, 1963), p. 213.
[17]J. W. Cooley and J. W. Tukey, Math. Comput. 19, 297 (1965).
[18]D. M. Pepper and A. Yariv, Opt. Lett. 5, 59 (1980).
[19]The authors are indebted to W. W. Rigrod for suggesting this type of substitution.
[20]E. T. Whittaker and G. N. Watson, *Modern Analysis* (Cambridge University Press, London, 1927), p. 355.